JOURNAL OF MAGNETIC RESONANCE Series B 111, 209–219 (1996)
ARTICLE NO. 0086

Microstructural and Physiological Features of Tissues Elucidated by Quantitative-Diffusion-Tensor MRI

PETER J. BASSER* AND CARLO PIERPAOLI†

*Biomedical Engineering and Instrumentation Program, NCRR, and †Neuroimaging Branch, NINDS, Building 13, Room 3N17, 13 South Drive, Bethesda, Maryland 20892-5766

Received April 7, 1995; revised January 31, 1996

Quantitative-diffusion-tensor MRI consists of deriving and displaying parameters that resemble histological or physiological stains, i.e., that characterize intrinsic features of tissue microstructure and microdynamics. Specifically, these parameters are objective, and insensitive to the choice of laboratory coordinate system. Here, these two properties are used to derive intravoxel measures of diffusion isotropy and the degree of diffusion anisotropy, as well as intervoxel measures of structural similarity, and fiber-tract organization from the effective diffusion tensor, $\mathbf{D}$, which is estimated in each voxel. First, $\mathbf{D}$ is decomposed into its isotropic and anisotropic parts, $\langle D \rangle \mathbf{I}$ and $\mathbf{D} - \langle D \rangle \mathbf{I}$, respectively (where $\langle D \rangle = \text{Trace}(\mathbf{D})/3$ is the mean diffusivity, and $\mathbf{I}$ is the identity tensor). Then, the tensor (dot) product operator is used to generate a family of new rotationally and translationally invariant quantities. Finally, maps of these quantitative parameters are produced from high-resolution diffusion tensor images (in which $\mathbf{D}$ is estimated in each voxel from a series of 2D-FT spin-echo diffusion-weighted images) in living cat brain. Due to the high inherent sensitivity of these parameters to changes in tissue architecture (i.e., macromolecular, cellular, tissue, and organ structure) and in its physiologic state, their potential applications include monitoring structural changes in development, aging, and disease.

INTRODUCTION

Diffusion-tensor MRI (DT-MRI) is an MR imaging modality that provides unique microstructural and physiological information [contained in the six independent components of the diffusion tensor, $\mathbf{D}$, and the T_2-weighted amplitude, $A(0)$]. DT-MRI also presents new challenges, one of which is to extract and display this information. One approach we used previously was to construct three-dimensional fiber maps and diffusion ellipsoid images (*1*) which highlight the three-dimensional character of diffusion in tissues and other media. Another approach, which we employ here, is to summarize (or contract) the information embodied in the six independent elements of $\mathbf{D}$ by deriving a new set of *scalar* quantities that measure distinct, intrinsic microstructural features of diffusion within tissues (and other media) with which we can help assess its physiologic state.

Quantitative-diffusion-tensor MRI, which we introduce here, consists of deriving and displaying new quantitative scalar parameters (from the effective diffusion tensor, $\mathbf{D}$) that measure different intrinsic features of heterogeneous, anisotropic media. These imaging parameters characterize diffusion isotropy, diffusion anisotropy, macrostructural similarity, and fiber-tract organization. We call them "quantitative" because each parameter behaves like a quantitative histological or physiological stain.[1] In addition, we establish general criteria and a framework for constructing other intrinsic quantitative imaging parameters from the diffusion tensor.

MRI parameters that are now used to characterize diffusion in anisotropic media are not quantitative. Specifically, they are exquisitely sensitive to the choice of the laboratory coordinate system and to the applied imaging and diffusion gradient pulse sequences. As a result, they have little value in drug evaluation studies, multisite studies, or retrospective studies of a single patient. Quantitative diffusion tensor MRI overcomes these deficiencies.

When the translational mobility of a diffusing molecule depends upon a medium's orientation, diffusion is anisotropic. In biological tissues such as brain white matter, skeletal muscle, kidney, and cardiac muscle [e.g., see (*2*)], we ascribe anisotropic diffusion (as measured by MR spectroscopy or imaging) to the presence of heterogeneous but spatially ordered macromolecular, membranous, and cellular compartments. On the scale of a macroscopic voxel, it is appropriate to use an effective diffusion tensor, $\mathbf{D}$, to characterize diffusion anisotropy (*3*). In such anisotropic media, we use diffusion tensor MRI (*1*) to estimate an effective diffusion tensor in each voxel, as well as to calculate its principal (orthotropic) directions and principal diffusivities. The former are the mutually perpendicular, preferred directions along which molecular displacements of the spin-labeled molecules are uncorrelated, while the latter are the diffusivities along these preferred directions. We then use

[1] The use of the term "stain" in connection with an NMR contrast mechanism was first brought to our attention by Professor G. Allan Johnson.

1064-1866/96 $18.00

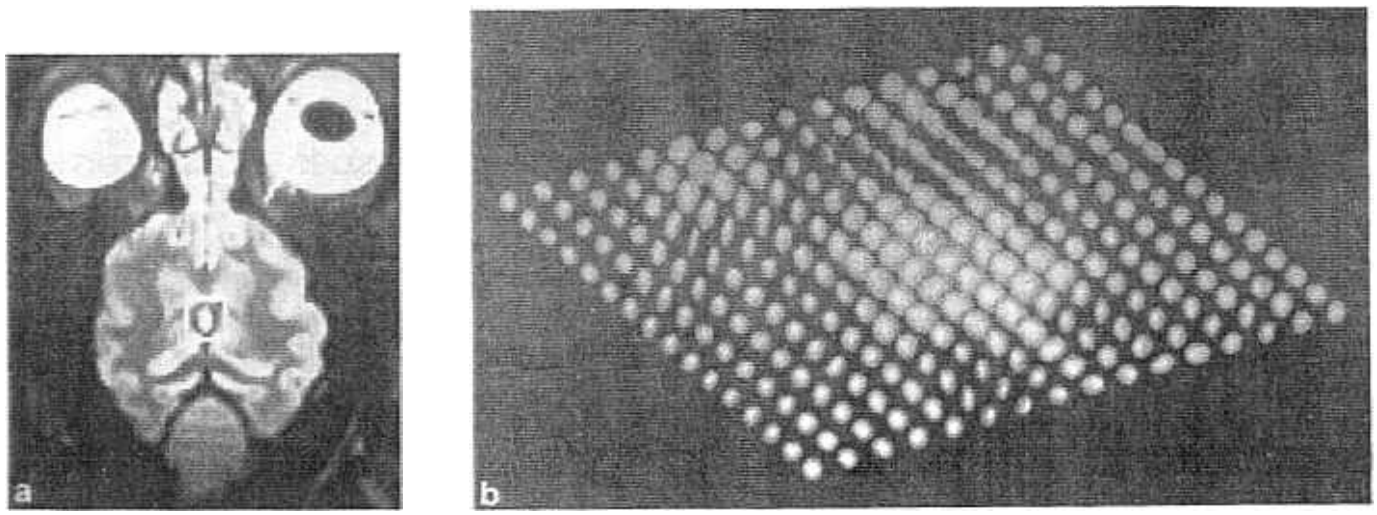

FIG. 1. (a) T_2-weighted image showing regions of gray matter, white matter, and CSF-filled ventricles in *in vivo* cat brain. (b) Diffusion ellipsoid image constructed from the effective diffusion tensor, $\underline{D}$, estimated in each voxel for the ROI enclosed by the white rectangle.

these quantities to derive measures of diffusion isotropy, diffusion anisotropy, macrostructural similarity, and fiber-tract organization.

To make the qualitative differences between these terms clear, consider the T_2-weighted image of living cat brain in Fig. 1a and the corresponding diffusion ellipsoid image (constructed for an ROI containing the internal capsule) in Fig. 1b. In principle, an image of a diffusion anisotropy index of this ROI should show the same contrast in voxels containing similar types of white matter, irrespective of their fiber-tract direction. This is because an anisotropy index should measure the degree of preferential mobility within a voxel, but should be insensitive to the direction along which diffusion is preferred. Geometrically, it should characterize the shape of the diffusion ellipsoid, but not its size or orientation. A measure of macrostructural (diffusive) similarity should identify tissues with a similar microstructure, specifically with similar principal directions and principal diffusivities. We expect that such a measure would be large in gray matter and larger still in the CSF-filled ventricles (where diffusion is largely isotropic), but it would not necessarily be large in regions containing white-matter fibers whose fiber direction is changing. Geometrically, a measure of structural similarity should measure the similarity of the shape, size, and orientation of different diffusion ellipsoids. Our definition of fiber-tract organization combines notions of diffusion anisotropy and macrostructural similarity. Fiber-tract organization is a property that we wish to ascribe only to anisotropic media (like white matter) but not to isotropic media (like the CSF-filled ventricles or most gray matter). Essentially, this parameter should measure the macrostructural similarity of the anisotropic part of the diffusion tensor in different voxels. Such a measure should highlight regions like the corpus callosum or the optical tract (where white-matter fiber tracts are packed in orderly bundles), but should show no fiber-tract organization in voxels containing isotropic media, such as gray matter and CSF-filled ventricles. In summary, these new one-dimensional (scalar) measures would provide new information about the three-dimensional character of diffusion in anisotropic tissues, information that has not been available using other MRI techniques.

We expect these parameters to be useful in elucidating structural features in normal, diseased, or degenerating tissues. The transformation of less-ordered to ordered, complex structures is a characteristic of normal development. This transformation occurs at a variety of length scales, including macromolecular (e.g., in neurofilaments and microtubules), cellular (e.g., in axons), tissue (e.g., in skeletal muscle, tendons, ligaments, and lens), and organ (e.g., in brain white matter, heart, and kidney). Moreover, preliminary findings that diffusion-weighted images are sensitive to architectural changes in the optic nerve prior to myelin deposition (*4*) suggest that these new parameters could be useful in assessing and characterizing normal and pathological developmental processes. Interest continues to grow in assessing developmental changes, particularly when induced by genetic manipulation or environmental stress. Noninvasive and nondestructive MRI techniques that can sense these changes may become increasingly valuable in such basic studies.

Conversely, the loss or lack of organization and structure at the molecular, cellular, tissue, and organ length scales is a characteristic of abnormal development, aging, or degeneration. For example, cardiac muscle fiber disorganization accompanies idiopathic cardiac myopathy and is believed to contribute to the loss of mechanical stiffness and pumping efficiency of the heart (*5*). A measure of the degree of fiber disorganization may be useful in diagnosing such pathologies, as also described by Wedeen *et al.* (*6*). Tumors in

white matter and muscle are also more disorganized than the surrounding normal tissues; a parameter that measures fiber organization may help to demarcate (segment) these domains. Therefore, objective parameters that measure microstructural features nondestructively and noninvasively may also be of clinical use.

BACKGROUND

Several different scalar indices derived from diffusion-weighted images (DWIs) have been used to characterize diffusion anisotropy. Moseley *et al.* (*7*) characterized diffusion anisotropy in each voxel by the ratio of differences and sums of DWIs with diffusion-sensitizing gradients applied in two perpendicular directions, e.g., x and y:

$$\frac{DWIx - DWIy}{DWIx + DWIy} \quad [1]$$

Douek *et al.* (*8*) characterized diffusion anisotropy in a voxel by the ratio of two apparent diffusion constants (ADCs), measured with diffusion-sensitizing gradients applied in two perpendicular directions, e.g., x and y,

$$\frac{ADC_x}{ADC_y}$$

and displayed as a color image (*8*). In voxels containing one particular tissue (such as white matter) when this ratio was a maximum, its value was assumed to be $ADC_\perp/ADC_\parallel$—the ratio of ADCs perpendicular to and parallel to the fiber-tract direction (*9*). Recently, van Gelderen *et al.* (*10*) proposed a scalar anisotropy index that is proportional to the standard deviation of three ADCs measured in three mutually perpendicular directions: ADC_x, ADC_y, and ADC_z, divided by their mean value, $\langle ADC \rangle$ (*10*),

$$\frac{\sqrt{(ADC_x - \langle ADC \rangle)^2 + (ADC_y - \langle ADC \rangle)^2 + (ADC_z - \langle ADC \rangle)^2}}{\langle ADC \rangle} \quad [3a]$$

where

$$\langle ADC \rangle = \frac{ADC_x + ADC_y + ADC_z}{3} \quad [3b]$$

Unfortunately, none of these anisotropy measures is quantitative. Anisotropy measures based upon DWIs (like Eq. [1]) are inherently nonobjective; that is, their contrast does not correspond to a single meaningful physical or chemical variable or fundamental parameter, but to a complicated combination of them. This is usually true for anisotropy measures that use the ADC, since they are estimated from DWIs using a model that may assume diffusion is isotropic. Even so, these anisotropy measures suffer from a more serious failing: They inherently depend on (a) the choice of the laboratory frame of reference (i.e., the x, y, z coordinate system used to represent the directions of the static B field and the applied magnetic field gradients in an MR experiment); (b) the choice of the direction of the applied diffusion gradients used to acquire the DWIs; (c) the orientation and placement of the tissue sample within the magnet; and (d) the orientation and position of the macromolecular, cellular, and/or fibrous structures within a voxel that produce the observed diffusion anisotropy.

Clearly, for an anisotropy index (or any other scalar measure of an intrinsic characteristic or feature) to possess the properties of a quantitative histological stain (such as an autoradiograph), it should be objective (i.e., its value in each voxel should be a known monotonic function of a meaningful physical quantity) and it should be invariant with respect to arbitrary rotations and translations. These intuitive criteria are used explicitly below to constrain the set of admissible scalar measures of structural features (such as diffusion anisotropy, structural similarity, and fiber organization) that we derive from the diffusion tensor.

THEORY

Measures of Isotropy and Anisotropy

Here we derive new quantitative parameters from the effective diffusion tensor, $\underline{\mathbf{D}}$, by employing tensor operations that to date have not been applied in MRI applications. First, we decompose $\underline{\mathbf{D}}$ into isotropic and anisotropic tensors:

$$\underline{\mathbf{D}} = \underbrace{\langle D \rangle \underline{\mathbf{1}}}_{\substack{\text{isotropic} \\ \text{tensor}}} + \underbrace{(\underline{\mathbf{D}} - \langle D \rangle \underline{\mathbf{1}})}_{\substack{\text{anisotropic} \\ \text{tensor}}} \quad [4]$$

Above, the isotropic part of $\underline{\mathbf{D}}$ is given by the (isotropic) identity tensor, $\underline{\mathbf{1}}$, multiplied by the (scalar) mean diffusivity, $\langle D \rangle$ (*11*), where

$$\langle D \rangle = \frac{\text{Trace}(\underline{\mathbf{D}})}{3} = \frac{D_{xx} + D_{yy} + D_{zz}}{3} = \frac{\lambda_1 + \lambda_2 + \lambda_3}{3}, \quad [5]$$

and where λ_1, λ_2, and λ_3 are the eigenvalues (or principal diffusivities) of $\underline{\mathbf{D}}$; and D_{xx}, D_{yy}, and D_{zz} are its diagonal elements measured in the laboratory frame of reference. We call the anisotropic part of $\underline{\mathbf{D}}$ the diffusion deviatoric or diffusion deviation tensor, $\underline{\mathbf{Q}}$:

$$\underline{\mathbf{Q}} = \underline{\mathbf{D}} - \langle D \rangle \underline{\mathbf{1}} \quad [6]$$

The term "deviatoric" is apt because $\underline{\mathbf{Q}}$ measures the deviation of $\underline{\mathbf{D}}$ from being an isotropic tensor, and is analogous

to the stress deviatoric (tensor) that is widely used in continuum mechanics and material sciences [e.g., see (*12*)]. The latter measures how the (symmetric) stress tensor deviates from the isotropic mean stress tensor. To form the stress deviatoric tensor, $\underline{\sigma}'$, the isotropic part of the stress tensor, $p\,\underline{1}$, is subtracted from the original stress tensor, $\underline{\sigma}$:

$$\underline{\sigma}' = \underline{\sigma} - \frac{\text{Trace}(\underline{\sigma})}{3}\underline{1} = \underline{\sigma} - p\underline{1}. \qquad [7]$$

We recognize p as either the hydrostatic pressure in a fluid or the mean stress in a solid. (One important difference between the stress and diffusion tensors, however, is that the latter must always be positive definite, whereas the former does not have to be). While this tensor decomposition is not unique, it is the most natural and physically motivated. (Appendix A shows that the eigenvalues of $\underline{\mathbf{D}}$ and $\underline{\mathbf{D}}'$ are simply related, and that both share the same eigenvectors or orthotropic directions.)

Having decomposed the diffusion tensor into its isotropic and anisotropic parts, we can obtain a (scalar) measure of their respective magnitudes (or lengths). Just as the magnitude of a vector $\mathbf{r}$ is given by the square root of its scalar dot product $\sqrt{\mathbf{r}\cdot\mathbf{r}}$, the magnitude of a tensor, such as $\underline{\mathbf{D}}$, is given by the square root of the (scalar) generalized tensor product or tensor dot product, $\sqrt{\underline{\mathbf{D}}:\underline{\mathbf{D}}}$ (*12*), where

$$\underline{\mathbf{D}}:\underline{\mathbf{D}} = \sum_{i=1}^{3}\sum_{j=1}^{3} D_{ij}^2 = \lambda_1^2 + \lambda_2^2 + \lambda_3^2 \qquad [8]$$

This generalized tensor product shares another property with the vector dot product: They both are independent of the position and orientation of the laboratory coordinate system in which their respective components are measured. In particular, $\underline{\mathbf{D}}:\underline{\mathbf{D}}$ (given in Eq. [8]) is a scalar invariant because it is a function solely of the eigenvalues of $\underline{\mathbf{D}}$, and because it is independent of their assignment or order (i.e., if we permute the subscripts of the eigenvalues, the value of an invariant quantity is unchanged.)

Referring to Eq. [6], we see that the magnitude or length of the isotropic part of $\underline{\mathbf{D}}$ is

$$\sqrt{\langle D\rangle\underline{1}:\langle D\rangle\underline{1}} = \langle D\rangle\sqrt{\underline{1}:\underline{1}} = \langle D\rangle\sqrt{3}, \qquad [9]$$

which is proportional to the scalar mean diffusivity, $\langle D\rangle$, whereas the magnitude of the anisotropic part of $\underline{\mathbf{D}}$ is given by

$$\sqrt{\underline{\mathbf{D}}':\underline{\mathbf{D}}'} = \sqrt{\sum_{i=1}^{3}\sum_{j=1}^{3}(D_{ij} - \langle D\rangle I_{ij})^2}. \qquad [10]$$

If we use Eq. [5] and exploit the symmetry of $\underline{\mathbf{D}}$ (i.e., thermodynamic considerations require that $\underline{\mathbf{D}} = \underline{\mathbf{D}}^T$), we can express Eq. [10] in the form

$$\sqrt{\underline{\mathbf{D}}':\underline{\mathbf{D}}'} = \sqrt{\begin{aligned}&(D_{xx} - \langle D\rangle)^2 + (D_{yy} - \langle D\rangle)^2\\ &+ (D_{zz} - \langle D\rangle)^2 + 2D_{xy}^2 + 2D_{xz}^2 + 2D_{yz}^2\end{aligned}}. \qquad [11]$$

The first three terms on the right-hand side of Eq. [11] are the sum of the squared deviations between the diagonal elements of $\underline{\mathbf{D}}$ and their mean value, $\langle D\rangle$; the remaining three terms are the sums of the squares of the off-diagonal elements of $\underline{\mathbf{D}}$. We see that $\sqrt{\underline{\mathbf{D}}':\underline{\mathbf{D}}'}$ is a scalar measure of the degree to which the diffusion tensor deviates from isotropy (in a mean-squared sense), so it is a natural basis for an anisotropy measure.

To show that $\underline{\mathbf{D}}':\underline{\mathbf{D}}'$ is a scalar invariant measure of anisotropy (just as Trace($\underline{\mathbf{D}}$) is a scalar invariant measure of isotropy), we express $\underline{\mathbf{D}}':\underline{\mathbf{D}}'$ in terms of the eigenvalues of $\underline{\mathbf{D}}$ [e.g., as in (*13*)]. In the principal frame, all off-diagonal elements of $\underline{\mathbf{D}}$ vanish (i.e., $D_{xy} = D_{xz} = D_{yz} = 0$) while all its diagonal elements, D_{xx}, D_{yy}, and D_{zz}, are replaced by the principal diffusivities, λ_1, λ_2, and λ_3. Equation [11] can be rewritten as

$$\begin{aligned}\sqrt{\underline{\mathbf{D}}':\underline{\mathbf{D}}'} &= \sqrt{(\lambda_1 - \langle D\rangle)^2 + (\lambda_2 - \langle D\rangle)^2 + (\lambda_3 - \langle D\rangle)^2}\\ &= \sqrt{3}\ \text{Var}(\lambda)\end{aligned}$$

This quantity is a scalar invariant. It is also the sum of the squares of the deviations between the principal diffusivities of $\underline{\mathbf{D}}$ and its mean diffusivity, $\langle D\rangle$ (see Eq. [5]), or alternatively, three times the sample variance of the three eigenvalues of $\underline{\mathbf{D}}$ within a voxel. For completeness, we can rewrite Eq. [12] (using Eq. [5] and a little algebra), as

$$\sqrt{\underline{\mathbf{D}}':\underline{\mathbf{D}}'} = \sqrt{\tfrac{1}{3}((\lambda_1 - \lambda_2)^2 + (\lambda_2 - \lambda_3)^2 + (\lambda_3 - \lambda_1)^2)}.$$

Taking the magnitude of the anisotropic part of $\underline{\mathbf{D}}$, and dividing it by the magnitude of the isotropic part of $\underline{\mathbf{D}}$, we obtain a measure of the relative anisotropy, RA:

$$\text{RA} = \frac{\sqrt{\underline{\mathbf{D}}':\underline{\mathbf{D}}'}}{\sqrt{\langle D\rangle\underline{1}:\langle D\rangle\underline{1}}} = \frac{1}{\sqrt{3}}\frac{\sqrt{\underline{\mathbf{D}}':\underline{\mathbf{D}}'}}{\langle D\rangle} = \frac{\sqrt{\text{Var}(\lambda)}}{\text{E}(\lambda)}$$

RA is quantitative (i.e., physically meaningful and invariant) and dimensionless. For an isotropic medium, RA = 0. RA also represents the ratio of the sample standard deviation [$\sqrt{\text{Var}(\lambda)}$] to the sample mean [$\text{E}(\lambda)$] of the three eigenvalues of $\underline{\mathbf{D}}$ in each voxel (λ).

Alternatively, we propose a measure of the fractional anisotropy, FA:

$$\mathrm{FA} = \sqrt{\frac{3}{2}}\frac{\sqrt{\mathbf{D}:\mathbf{D}}}{\sqrt{\mathbf{D}:\mathbf{D}}} \qquad [15]$$

The FA index measures the fraction of the "magnitude" of $\mathbf{D}$ that we can ascribe to anisotropic diffusion. Like RA, FA is quantitative and dimensionless. For an isotropic medium, FA = 0. For a cylindrically symmetric anisotropic medium (i.e., with $\lambda_1 \gg \lambda_2 = \lambda_3$), FA = 1. Pierpaoli *et al.* (*14*) recently presented images of the FA index in living human brain, which are bright in regions where there are anisotropic structures (such as the corpus callosum and the ventral internal capsule), but are dark in more isotropic regions (such as in gray matter and in CSF-filled ventricles).

Measures of Macrostructural Diffusive Similarity

So far, we have considered only *intravoxel* parameters, specifically quantities that characterize diffusion isotropy and anisotropy within a voxel. However, to measure macrostructural features, we must examine the pattern or distribution of diffusion tensors within an image volume. Such a measure might characterize the degree of macrostructural (diffusive) similarity. However, this requires intervoxel comparisons. Below, we show how to measure the similarity of diffusion tensors quantitatively.

Just as the dot product between two vectors measures their degree of similarity or colinearity, the generalized tensor (dot) product between two tensors measures their similarity. A reasonable measure of structural (diffusive) similarity between media in different voxels is $\sqrt{\mathbf{D}:\mathbf{D}'}$. However, to use this formula as a measure of (diffusive) similarity, we must demonstrate that it possesses the required properties of a quantitative measure (i.e., objectivity as well as translational and rotational invariance). These properties are demonstrated in Appendix B, where we also show that $\mathbf{D}:\mathbf{D}'$ can be expressed in terms of the eigenvalues (λ_k and λ'_s) and eigenvectors (ε_k and ε'_s) of $\mathbf{D}$ and $\mathbf{D}'$, respectively, i.e.,

$$\mathbf{D}:\mathbf{D}' = \sum_{k=1}^{3}\sum_{s=1}^{3} \lambda_k\lambda'_s(\varepsilon_k^{\mathrm{T}}\varepsilon'_s)^2 \qquad [16]$$

Geometrically, we can use Eq. [16] to devise scalar measures of the similarity of the size, shape, and orientation of two different diffusion ellipsoids constructed from $\mathbf{D}$ and $\mathbf{D}'$. Since all λ_k and λ'_s are positive, and so are $(\varepsilon_k^{\mathrm{T}}\varepsilon'_s)^2$, every term in Eq. [16] is positive. Note that the eigenvectors ε_k and ε'_s of two different diffusion tensors are generally not parallel or orthogonal to one another.

Now that we have developed an invariant quantity that measures the similarity of diffusion tensors in different voxels, we can construct new scalar images from the diffusion tensor image [i.e., the image in which every voxel contains an estimated diffusion tensor (*1*)]. To measure macrostructural similarity with respect to a particular reference voxel (with an effective diffusion tensor $\mathbf{D}$), we can form a similarity image by calculating the (scalar) matrix product, $\mathbf{D}:\mathbf{D}'$, where $\mathbf{D}'$ is the effective diffusion tensor in any arbitrary voxel. To obtain a measure of local similarity, we can sum the matrix products between the reference diffusion tensor, $\mathbf{D}(\mathbf{r})$, and those in other voxels, $\mathbf{D}(\mathbf{r}')$, weighting their scalar matrix products by a function of the distance between them. Since this measure is a weighted sum of scalar invariants, it too is a scalar invariant. A natural way to do this is to define a correlation measure of structural similarity, $S(\mathbf{r})$, by convolving $\mathbf{D}(\mathbf{r}):\mathbf{D}(\mathbf{r}')$ with a kernel, $K(\mathbf{r}-\mathbf{r}')$, integrating their product over the entire imaging volume, V:

$$S(\mathbf{r}) = \frac{1}{V}\frac{\int_V \mathbf{D}(\mathbf{r}):\mathbf{D}(\mathbf{r}')\,K(\mathbf{r}-\mathbf{r}')\,d\mathbf{r}'^3}{\mathbf{D}(\mathbf{r}):\mathbf{D}(\mathbf{r})}$$

With no a priori information, it is optimal to choose a normalized isotropic Gaussian convolution kernel (although other windows could be chosen if additional a priori information were available):

$$K(\mathbf{r}-\mathbf{r}') = \frac{1}{\sqrt{(2\pi\sigma^2)^3}}\exp\left(\frac{-(\mathbf{r}-\mathbf{r}')^{\mathrm{T}}(\mathbf{r}-\mathbf{r}')}{2\sigma^2}\right) \qquad [18]$$

We chose an isotropic convolution kernel so that no directional bias is introduced. We also require that the convolution kernel have an area equal to one, to normalize the result. This formula can be evaluated efficiently (even for 3-D data sets) using the convolution theorem of discrete Fourier transforms (*15*). Equation [18] extends the formalism introduced by Marr (*16*) to smooth images.

For discrete MR images, Eqs. [17] and [18] do not apply since the diffusion tensors are not continuous functions of position, but voxel-averaged quantities defined within each voxel. We must therefore replace the integral in Eq. [17] with a discrete sum over voxels within the image space:

$$S(\mathbf{r}) = \sum_l\sum_m\sum_n\left\{\sum_{k=1}^{3}\sum_{s=1}^{3}\lambda_k(\mathbf{r})\lambda_s(\mathbf{r}')[\varepsilon_k^{\mathrm{T}}(\mathbf{r})\varepsilon_s(\mathbf{r}')]^2\right\} \frac{1}{\sqrt{(2\pi\sigma^2)^3}}\exp\left(\frac{-(\mathbf{r}-\mathbf{r}')^{\mathrm{T}}(\mathbf{r}-\mathbf{r}')}{2\sigma^2}\right)\Delta x\Delta y\Delta z$$

having used the substitutions

$$\mathbf{r}' = (l\Delta x, n\Delta y, m\Delta z)^{\mathrm{T}};$$
$$\mathbf{r} = (i\Delta x, j\Delta y, k\Delta z)^{\mathrm{T}}; \text{ and}$$
$$d\mathbf{r}'^3 = \Delta x\Delta y\Delta z, \qquad [19b]$$

where Δx, Δy, and Δz represent the individual voxel dimensions. These definitions apply for both isotropic and anisotropic voxels. To mitigate errors introduced at the boundaries of the imaging volume, we can pad the multislice or 3-D images with zeros. The correlation length σ in Eq. [18] should now be at least as large as the smallest voxel dimension.

Fiber-Tract Organization Measures

To measure the degree of fiber-tract organization, we use a measure of the similarity between the anisotropic parts (or deviatorics) of diffusion tensors in different voxels, $\underline{\mathbf{D}}:\underline{\mathbf{D}}'$. In Appendix C we derive the generalized tensor product between the diffusion deviation tensors in a reference and an arbitrarily chosen voxel, $\underline{\mathbf{D}}:\underline{\mathbf{D}}'$, in terms of their eigenvectors and eigenvalues, obtaining

$$\underline{\mathbf{D}}:\underline{\mathbf{D}}' = \sum_{k=1}^{3}\sum_{s=1}^{3} \lambda_k\lambda_s'(\boldsymbol{\varepsilon}_k^T\boldsymbol{\varepsilon}_s')^2 - \tfrac{1}{3}\Big(\sum_{k=1}^{3}\lambda_k\Big)\Big(\sum_{s=1}^{3}\lambda_s'\Big). \quad [20]$$

Equivalently, Eq. [20] can be written as

$$\underline{\mathbf{D}}:\underline{\mathbf{D}}' = \mathbf{D}:\mathbf{D}' - 3\langle D\rangle\langle D'\rangle. \quad [21]$$

where we have used Eq. [5] above. Therefore, the tensor product between two diffusion deviation tensors is the tensor product between their respective diffusion tensors minus three times the product of their respective mean diffusivities. Since $\mathbf{D}:\mathbf{D}'$ and $\langle D\rangle\langle D'\rangle$ are both invariant, $\underline{\mathbf{D}}:\underline{\mathbf{D}}'$ is also invariant.

Now that we have defined an invariant measure of similarity for anisotropic structures, we can again apply the convolution averaging procedure used above to develop a measure of fiber organization. To retain information about local order (i.e., tissue domains with similar structure and orientation) within the vicinity of the reference voxel, we again weight the scalar matrix products between deviatorics in neighboring voxels more heavily than we do those between distant ones. By analogy, we define a correlation measure of organization, $O(\mathbf{r})$:

$$O(\mathbf{r}) = \frac{1}{V}\int_V \frac{\underline{\mathbf{D}}(\mathbf{r})}{\sqrt{\mathbf{D}(\mathbf{r}):\mathbf{D}(\mathbf{r})}} : \frac{\underline{\mathbf{D}}(\mathbf{r}')}{\sqrt{\mathbf{D}(\mathbf{r}'):\mathbf{D}(\mathbf{r}')}} \times K(\mathbf{r}-\mathbf{r}')[1-\delta(\mathbf{r}-\mathbf{r}')]d\mathbf{r}'^3 \quad [22]$$

The normalization of the deviatorics in the integrand guarantees that the anisotropic macrostructural similarity index will always lie between 0 and 1, with 0 indicating no order and 1 indicating a locally uniform fiber-tract pattern. The tensor product in the integrand of Eq. [22] now resembles a correlation coefficient. The term containing the delta function, $[1-\delta(\mathbf{r}-\mathbf{r}')]$, eliminates the contribution produced by the inner product of the reference deviatoric with itself, $\underline{\mathbf{D}}(\mathbf{r}):\underline{\mathbf{D}}(\mathbf{r})$. Since $O(\mathbf{r})$ is a weighed sum of scalar invariants, it too is a scalar invariant. It can also be displayed as an image whose intensity should be large where the fiber-tract direction field is regular or relatively uniform. For example, in normal brain, we would expect a gray-scale image of $O(\mathbf{r})$ to be bright in organized regions (such as the corpus callosum and the optical tract), and dark in less-organized regions (such as fluid-filled ventricles, in gray matter, and even some more-disordered regions of white matter).

For MR images, we replace the integral with a sum over discrete voxels in the image space

$$O(\mathbf{r}) = \sum_i\sum_m\sum_n \left\{\sum_{k=1}^{3}\sum_{s=1}^{3}\lambda_k(\mathbf{r})\lambda_s(\mathbf{r}')[\boldsymbol{\varepsilon}_k^T(\mathbf{r})\boldsymbol{\varepsilon}_s(\mathbf{r}')]^2 - \frac{1}{3}\sum_{k=1}^{3}\lambda_k(\mathbf{r})\sum_{s=1}^{3}\lambda_s(\mathbf{r}')\right\} \times \frac{1}{\sqrt{(2\pi)^3\sigma^2}}\exp\left(\frac{-(\mathbf{r}-\mathbf{r}')^T(\mathbf{r}-\mathbf{r}')}{2\sigma^2}\right) \times -\delta(\mathbf{r}-\mathbf{r}'))\Delta x\Delta y\Delta z \quad [23]$$

and use the substitutions in Eq. [19b] above.

MATERIALS AND METHODS

MR data were obtained with a General Electric 2.0 T Omega MR system (GE NMR Instruments, Fremont, California) equipped with self-shielded gradients (Acustar 290) capable of producing pulses up to 4.0 G/cm. A homebuilt quadrature coil (13 cm diameter) was used as a radiofrequency transmitter and receiver. We acquired 21 axial multislice diffusion-weighted 2D spin-echo images of living cat brain in under 3 h. Imaging acquisition parameters were as follows: four axial slices, 2 mm slice thickness, TR/TE of 2000/70, two repetitions per image, 90 mm field of view, 40 kHz bandwidth, 128 × 256 in-plane resolution. Different levels of diffusion weighting were obtained by varying the strength of pairs of trapezoidal gradient pulses placed on both sides of the 180° pulse between 0 and 3 G/cm (*17–19*). The diffusion sensitizing gradients had a duration of 19 ms and were separated by a time interval of 20 ms. The highest *b*-matrix values were on the order of 850 s/mm^2. Diffusion gradients were applied in seven noncollinear directions (*20*). From the measured T_2-weighted signal, A(TE), and the *b* matrix calculated from each sequence (*21*), we estimated $\mathbf{D}$ in each voxel, using weighted multivariate linear regression of (*20*):

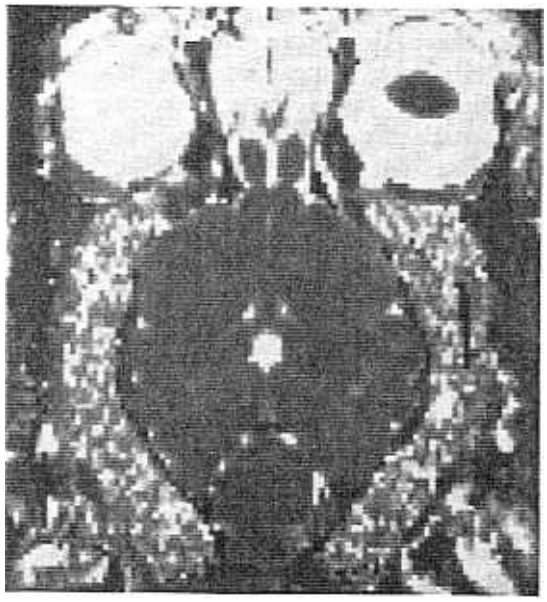

FIG. 2. Image of Trace($\underline{D}$) for cat brain, calculated using Eq. [5]. Trace($\underline{D}$) arises naturally as an invariant imaging parameter from the decomposition of the effective diffusion tensor into its isotropic and anisotropic parts, as in Eq. [4].

$$\ln\left(\frac{A(TE)}{A(0)}\right) = -\sum_{i=1}^{3}\sum_{j=1}^{3} b_{ij}D_{ij}. \qquad [24]$$

The indices above were calculated from $\underline{D}$ estimated in each voxel.

EXPERIMENTAL RESULTS AND DISCUSSION

Figure 2 shows the isotropic part of the diffusion tensor, Trace($\underline{D}$) in cat brain, calculated from $\underline{D}$ in each voxel using Eq. [5]. Figure 3 shows the fractional anisotropy index, Eq. [15], calculated from $\underline{D}$ in each voxel. Figure 4 shows the organization index, Eq. [23] calculated from the series of multislice images. For ease of implementation, we used a rectangular window including only nearest neighbor voxels rather than the Gaussian window suggested above.

One of the novel contributions of this work is the use of the tensor decomposition (Eq. [4]) and the tensor product (e.g., in Eq. [8]) to derive intrinsic parameters characterizing features of isotropic and anisotropic diffusion in tissues and other media. This approach also provides a unified conceptual framework with which to present these invariant parameters.

The first parameter that arises naturally from this decomposition is the magnitude of the isotropic part of $\underline{D}$, $\langle D \rangle$ (see Eq. [5]), the mean diffusivity obtained by averaging the translational displacement distribution uniformly in all directions (*11*). We first proposed this invariant quantity as a useful MRI parameter whose value is independent of the orientation of anisotropic structures within a voxel (*22*). Figure 2 shows an image of Trace($\underline{D}$) = 3 $\langle D \rangle$ for the live cat.

FIG. 3. The fractional anisotropy index, Eq. [15], evaluated from the estimated effective diffusion tensor in each voxel.

The invariant relative anisotropy index given in Eq. [14] embodies the three-dimensional character of diffusion anisotropy. It is particularly instructive to compare this index

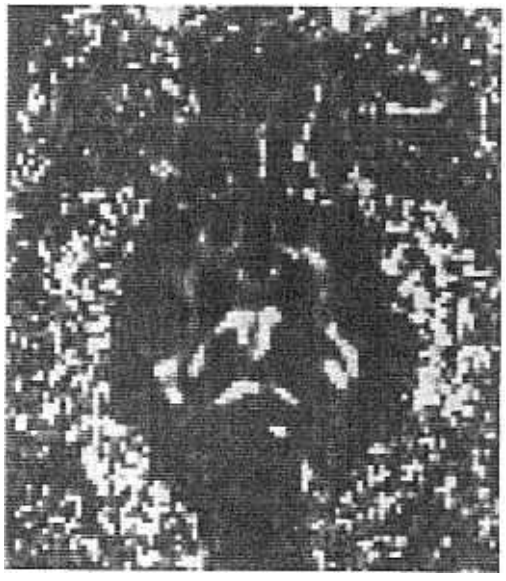

FIG. 4. The organization index (Eq. [23]) evaluated using three contiguous axial slices of *in vivo* cat brain. The image was implemented using a simplified algorithm in which the convolution kernel was a box function that included only nearest-neighbor voxels.

to the "SD" anisotropy measure proposed by van Gelderen *et al.* (Eqs. [3a], [3b]), which is not rotationally or translationally invariant. The primary difference between these two measures is that Eq. [14] contains the sum of the squares of the off-diagonal elements of $\mathbf{D}$, whereas Eqs. [3a], [3b] do not. (One can see this by comparing $\mathbf{D}:\mathbf{D}$ in Eq. [11] and the numerator in Eq. [3a]). From this, we predict that the SD measure of anisotropy will depend on the orientation of the anisotropic structures with respect to the laboratory coordinate frame, and thus will introduce an artifact into the measurement of anisotropy that depends upon orientation. Based upon the form of Eq. [3a], we can even predict how this artifact will manifest itself. The error in the SD measure will be smaller for anisotropic structures that lie parallel to one of the laboratory coordinate (x–y–z) axes, but may be as large as 100% for structures oriented obliquely to all of the coordinate axes, making those anisotropic structures appear almost isotropic.

Generally, knowing the ADCs measured in any three orthogonal directions (as in Eqs. [3a], [3b]) is not sufficient to characterize diffusion anisotropy. By examining the form of the scalar invariant $\mathbf{D}:\mathbf{D}$ in Eq. [12], and the anisotropy measures we propose in Eqs. [14] and [15], we see that to characterize diffusion anisotropy adequately requires at least knowing the three eigenvalues of $\mathbf{D}$. Since in most MRI applications we do not determine them a priori, we must generally resort to calculating them from the diagonal and off-diagonal elements of the estimated diffusion tensor, $\mathbf{D}$ (*1, 20*).

Equation [20] has an interesting potential application: It could be used to discriminate between different structural/architectural motifs, such as between isotropically or anisotropically packed fibers, or between flat or twisted fiber sheets (in which, for example, ε_2 and ε_3 rotate around ε_1). This application may be of use in elucidating fiber architectural motifs in the heart (*6, 23*).

The organizational index, shown in Fig. 4, shows high contrast in the corpus callosum and ventral internal capsules, where we know that the nerve fiber tracts run parallel to each other. In cortical regions containing white matter, the contrast is lower. Anatomically, these are regions in which we know the fiber patterns are less coherent. There is virtually no observed contrast in the gray matter or in the CSF-filled ventricles, where there is effectively no macroscopic organization.

While the scalar invariant MRI parameters are insensitive to the orientation of the sample, to the orientation of the gradients, and to the laboratory coordinate system, they may be affected by other independent parameters in the NMR experiment, such as voxel dimension. When we discretize the structural similarity and fiber organization measures (as in Eqs. [19a] and [23a]), we introduce a new length scale: the characteristic length of the voxel. These invariant measures are not guaranteed to be independent of voxel size, so we must specify it when using them. It will be interesting to study systematically how these measures of isotropy, anisotropy, similarity, and organization in tissues and other media are affected by voxel size (e.g., in microscopic diffusion tensor imaging studies) (*24*). Finally, if the voxel dimensions are not significantly smaller than the regions in which there are distinct tissue types, then their correlation length, σ, will always be too large to resolve any local order or structural similarity. Such is the case in the corpus callosum in Fig. 4.

Although it does possess the required properties of a quantitative MRI parameter, we do not want to leave the impression that the invariant organizational measure proposed in Eq. [23] is the only admissible measure of local order. Other measures, including some based on the Shannon information (*25*), are attractive. However, to estimate them requires segmenting a high-dimensional parameter space; ironically, this leaves us with the same problem that we posed in the Introduction—to reduce the complexity of a high-dimensional data set like the diffusion tensor image.

CONCLUSIONS

One of our aims has been to propose new and useful MRI parameters that behave as physiological or histological "stains", as well as a formal prescription for deriving them from the effective diffusion tensor, $\mathbf{D}$. The specific parameters we propose stain for intrinsic structural and physiological features such as diffusion isotropy, diffusion anisotropy, structural similarity, and fiber-tract organization. A quantitative physiological stain must be insensitive to an arbitrary rotation and translation of the laboratory coordinate system. We show that to characterize diffusion anisotropy (*26*), we must at least know all three eigenvalues of $\mathbf{D}$, and that to characterize the degree of structural similarity or fiber-tract organization adequately, we must know both the eigenvalues and eigenvectors of $\mathbf{D}$ (and those in surrounding voxels). This information can be calculated directly using all elements (i.e., both diagonal and off-diagonal elements) of the estimated diffusion tensor, $\mathbf{D}$, but cannot be calculated from the apparent diffusion coefficients, ADCs obtained in two or three orthogonal directions. In general, measurements based upon ADCs obtained in two or three orthogonal directions cannot be used to assess tissue anisotropy quantitatively, or any other feature that is related to it.

In previous studies, it has been demonstrated that with fast diffusion-weighted imaging sequences, such as high-resolution diffusion-weighted EPI (*27*), we can measure an effective diffusion tensor, $\mathbf{D}$, *in vivo* in each voxel in under 30 min (*14*), a reasonable period in which to make a clinical assessment. The new imaging parameters proposed above can be calculated from $\mathbf{D}$ in each voxel almost instantly, using conventional software packages. Therefore, as fast imagers become more widely available, so should one's ability

to glean new structural and physiological information calculated from diffusion tensor images.

APPENDIX A

It is easy to show that the isotropic part of $\underline{\mathbf{D}}$ vanishes (i.e., its trace is zero). This can be demonstrated using Eqs. [5] and [6]:

$$\begin{aligned}\text{Trace}(\underline{\mathbf{D}}) &= \text{Trace}(\underline{\mathbf{D}}) - \langle D\rangle \text{Trace}(\underline{\mathbf{I}}) \\ &= 3\langle D\rangle - 3\langle D\rangle = 0.\end{aligned}$$

In addition, the eigenvalues of $\underline{\mathbf{D}}$ and $\underline{\mathbf{D}}$ are related. The eigenvalues of $\underline{\mathbf{D}}$ are determined from the characteristic equation:

$$|\underline{\mathbf{D}} - \lambda \underline{\mathbf{I}}| = 0 \qquad [A2]$$

whereas the eigenvalues for $\underline{\mathbf{D}}$ are given by

$$\begin{aligned}|\underline{\mathbf{D}} - \lambda' \underline{\mathbf{I}}| &= |\underline{\mathbf{D}} - \langle D\rangle \underline{\mathbf{I}} - \lambda' \underline{\mathbf{I}}| \\ &= |\underline{\mathbf{D}} - (\langle D\rangle + \lambda')\underline{\mathbf{I}}| = 0. \qquad [A3]\end{aligned}$$

Equations [A2] and [A3] show that the characteristic equations for $\underline{\mathbf{D}}$ and $\underline{\mathbf{D}}$ are identical, except that the eigenvalues of $\underline{\mathbf{D}}$ and $\underline{\mathbf{D}}$, λ and λ', respectively, differ by the mean diffusivity, $\langle D\rangle$, i.e.,

$$\lambda = \langle D\rangle + \lambda' \text{ or } \lambda' = \lambda - \langle D\rangle \qquad [A4]$$

It follows directly that $\underline{\mathbf{D}}$ and $\underline{\mathbf{D}}$ also possess the same eigenvectors, ε_i, since in both cases we must solve the same set of matrix equations to obtain them,

$$(\underline{\mathbf{D}} - \lambda_i \underline{\mathbf{I}})\varepsilon_i = 0 \qquad [A5]$$

This means that these two tensors share the same principal or orthotropic directions.

APPENDIX B

To express $\underline{\mathbf{D}}:\underline{\mathbf{D}}'$ in terms of the eigenvalues and eigenvectors of $\underline{\mathbf{D}}$ and $\underline{\mathbf{D}}'$, we first diagonalize them according to

$$\underline{\mathbf{D}} = \underline{\mathbf{E}}\underline{\Delta}\underline{\mathbf{E}}^{\mathrm{T}}; \quad \underline{\mathbf{D}}' = \underline{\mathbf{E}}'\underline{\Delta}'\underline{\mathbf{E}}'^{\mathrm{T}} \qquad [B1a]$$

where $\underline{\mathbf{E}}$ and $\underline{\mathbf{E}}'$ are matrices whose columns are the orthonormal eigenvectors of $\underline{\mathbf{D}}$ and $\underline{\mathbf{D}}'$, respectively, i.e.,

$$\underline{\mathbf{E}} = (\varepsilon_1|\varepsilon_2|\varepsilon_3); \quad \underline{\mathbf{E}}' = (\varepsilon_1'|\varepsilon_2'|\varepsilon_3') \qquad [B1b]$$

and where $\underline{\Delta}$ and $\underline{\Delta}'$ are the diagonal matrices containing the eigenvalues of $\underline{\mathbf{D}}$ and $\underline{\mathbf{D}}'$, respectively:

$$\underline{\Delta} = \begin{pmatrix}\lambda_1 & 0 & 0\\ 0 & \lambda_2 & 0\\ 0 & 0 & \lambda_3\end{pmatrix}; \underline{\Delta}' = \begin{pmatrix}\lambda_1' & 0 & 0\\ 0 & \lambda_2' & 0\\ 0 & 0 & \lambda_3'\end{pmatrix} \qquad [B1c]$$

Here, it is convenient to introduce index notation and the Einstein summation convention (*28*) (i.e., any index appearing twice in an expression is automatically summed over the range of values that index assumes). Using Eq. [B1a], we can rewrite $\underline{\mathbf{D}}:\underline{\mathbf{D}}'$ as

$$\underline{\mathbf{D}}:\underline{\mathbf{D}}' = D_{ij}D_{ij}' = E_{ik}\Lambda_{kl}E_{jl}E_{is}'\Lambda_{sr}'E_{jr}' \qquad [B2]$$

Since, Δ and Δ' are diagonal matrices, we can rewrite Eq. [B1c] as

$$\Lambda_{kl} = \lambda_k\delta_{kl} \text{ and } \Lambda_{sr}' = \lambda_s'\delta_{sr}$$

(no summation over s and k !) [B3a,b]

where δ_{pq} is the Kronecker delta (*28*). Substituting Eq [B3a,b] into [B2] and simplifying, we obtain

$$\underline{\mathbf{D}}:\underline{\mathbf{D}}' = E_{ik}\lambda_k\delta_{kl}E_{jl}E_{is}'\lambda_s'\delta_{sr}E_{jr}' = \lambda_kE_{ik}E_{jk}\lambda_s'E_{is}'E_{jr}' \qquad [B4]$$

By commuting and regrouping terms, Eq. [B4] becomes

$$\begin{aligned}\underline{\mathbf{D}}:\underline{\mathbf{D}}' &= \lambda_k\lambda_s'(E_{ik}E_{is}')(E_{jk}E_{jr}') \\ &= \lambda_k\lambda_s'(E_{ki}^{\mathrm{T}}E_{is}')(E_{rj}^{\mathrm{T}}E_{jr}') \qquad [B5]\end{aligned}$$

The quantities in parentheses above represent the dot product between eigenvectors of $\underline{\mathbf{D}}$ and $\underline{\mathbf{D}}'$. Since j and i are dummy indices, these dot products can be rewritten as

$$E_{ki}^{\mathrm{T}}E_{is}' = E_{rj}^{\mathrm{T}}E_{jr}' = \varepsilon_k^{\mathrm{T}}\varepsilon_s' \qquad [B6]$$

Now using Eq. [B6], Eq. [B5] becomes

$$\underline{\mathbf{D}}:\underline{\mathbf{D}}' = \lambda_k\lambda_s'(\varepsilon_k^{\mathrm{T}}\varepsilon_s')^2 = \sum_{k=1}^{3}\sum_{s=1}^{3}\lambda_k\lambda_s'(\varepsilon_k^{\mathrm{T}}\varepsilon_s')^2, \qquad [B7]$$

which is what we set out to show.

Now, to show that $\underline{\mathbf{D}}:\underline{\mathbf{D}}'$ is an invariant quantity, we need only show that the right-hand side of Eq. [B7] is invariant. Although it is well known that all eigenvalues of a symmetric matrix are invariant under any proper rotation of the laboratory coordinate system [for a proof see (*29*)], we still must show that $\varepsilon_k^{\mathrm{T}}\varepsilon_s'$ is invariant. This seems clear from geometrical considerations and is also easy to demonstrate algebraically.

If $\underline{\mathbf{A}}$ is a transformation matrix between eigenvectors in two laboratory frames

$$\underline{\mathbf{A}}\boldsymbol{\varepsilon}_k^0 = \boldsymbol{\varepsilon}_k \text{ and } \underline{\mathbf{A}}\boldsymbol{\varepsilon}_s'^0 = \boldsymbol{\varepsilon}_s', \quad [B8]$$

and $\underline{\mathbf{A}}$ is a proper orthogonal transformation (*30*), i.e.,

$$\underline{\mathbf{A}}^T\underline{\mathbf{A}} = \underline{\mathbf{A}}^{-1}\underline{\mathbf{A}} = \underline{\mathbf{I}}, \quad [B9]$$

then the inner (dot) product of the eigenvectors is the same in both frames:

$$\begin{aligned}\boldsymbol{\varepsilon}_k^T\boldsymbol{\varepsilon}_s' &= (\underline{\mathbf{A}}\boldsymbol{\varepsilon}_k^0)^T(\underline{\mathbf{A}}\boldsymbol{\varepsilon}_s'^0) = \boldsymbol{\varepsilon}_k^{0T}\underline{\mathbf{A}}^T\underline{\mathbf{A}}\boldsymbol{\varepsilon}_s'^0 \\ &= \boldsymbol{\varepsilon}_k^{0T}\underline{\mathbf{I}}\boldsymbol{\varepsilon}_s'^0 = \boldsymbol{\varepsilon}_k^{0T}\boldsymbol{\varepsilon}_s'^0. \quad [B10]\end{aligned}$$

This equation also demonstrates that $\boldsymbol{\varepsilon}_k^T\boldsymbol{\varepsilon}_s'$ is invariant for all s and k, and thus $\underline{\mathbf{D}}:\underline{\mathbf{D}}'$ is invariant.

APPENDIX C

First, using the Einstein summation convention, we write $\underline{\mathbf{D}}:\underline{\mathbf{D}}'$ as

$$\underline{\mathbf{D}}:\underline{\mathbf{D}}' = D_{ij}D_{ij}' = \left(D_{ij} - \frac{D_{kk}}{3}\delta_{ij}\right)\left(D_{ij}' - \frac{D_{ww}'}{3}\delta_{ij}\right)$$

When expanded, this expression becomes

$$\underline{\mathbf{D}}:\underline{\mathbf{D}}' = D_{ij}D_{ij}' - \frac{1}{3}D_{kk}D_{ij}'\delta_{ij} - \frac{1}{3}D_{ww}'D_{ij}\delta_{ij} + \frac{D_{kk}'}{3}\frac{D_{ww}}{3}\delta_{ij}\delta_{ij} \quad [C2]$$

Since

$$\begin{aligned}&\delta_{ij}\delta_{ij} = 3 = \text{Trace}(\underline{\mathbf{I}}); \quad D_{ij}\delta_{ij} = D_{ii} = \text{Trace}(\underline{\mathbf{D}}); \\ &D_{ij}'\delta_{ij} = D_{ii}' = \text{Trace}(\underline{\mathbf{D}}'), \quad [C3]\end{aligned}$$

Eq. [C2] reduces to

$$\underline{\mathbf{D}}:\underline{\mathbf{D}}' = D_{ij}D_{ij}' - \frac{1}{3}D_{kk}D_{ww}' = \underline{\mathbf{D}}:\underline{\mathbf{D}}' - 3\langle D\rangle\langle D'\rangle, \quad [C4]$$

where we have used Eq. [5] above. Therefore, the matrix product of two diffusion deviation tensors is merely the matrix product of their respective diffusion tensors less three times the product of their respective mean diffusivities.

Since Trace($\underline{\mathbf{D}}$) and Trace($\underline{\mathbf{D}}'$) are both invariant quantities,

$$D_{kk} = \sum_{k=1}^{3} D_{kk} = \sum_{k=1}^{3}\lambda_k \quad \text{and} \quad D_{ww}' = \sum_{w=1}^{3} D_{ww}' = \sum_{s=1}^{3}\lambda_s', \quad [C5]$$

we can now use Eqs. [C5] and Eq. [16] to write Eq. [C4] in terms of the eigenvectors and eigenvalues of $\underline{\mathbf{D}}$ and $\underline{\mathbf{D}}'$, as in Eq. [20].

ACKNOWLEDGMENTS

This paper is dedicated to the memory of Hyung Goo Kim (1957–1995). The authors thank Barry Bowman for editing this manuscript.

REFERENCES

1. P. J. Basser, J. Mattiello, and D. Le Bihan, *Biophys. J.* **66**, 259 (1994).
2. R. M. Henkelman, G. J. Stanisz, J. K. Kim, and M. J. Bronskill, *Magn. Reson. Med.* **32**, 592 (1994).
3. J. Crank, "The Mathematics of Diffusion," second ed., p. 414, Oxford Univ. Press, Oxford, 1975.
4. D. M. Wimberger, T. P. Roberts, A. J. Barkovich, L. M. Prayer, M. E. Moseley, and J. Kucharczyk, *J. Comput. Assist. Tomogr.* **19**, 28 (1995).
5. K. T. Weber, C. G. Brilla, and J. S. Janicki, *Cardiovasc. Res.* **27**, 341 (1993).
6. V. J. Wedeen, T. G. Reese, R. N. Smith, and B. R. Rosen, *in* "SMR/ESMRMB Joint Meeting, Nice, France, 1995," p. 357.
7. M. E. Moseley, Y. Cohen, J. Kucharczyk, J. Mintorovitch, H. S. Asgari, M. F. Wendland, J. Tsuruda, and D. Norman, *Radiology* **176**, 439 (1990).
8. P. Douek, R. Turner, J. Pekar, N. Patronas, and D. Le Bihan, *J. Comput. Assist. Tomogr.* **15**, 923 (1991).
9. G. G. Cleveland, D. C. Chang, C. F. Hazlewood, and H. E. Rorschach, *Biophys. J.* **16**, 1043 (1976).
10. P. van Gelderen, M. H. M. d. Vleeschouwer, D. DesPres, J. Pekar, P. C. M. v. Zijl, and C. T. W. Moonen, *Magn. Reson. Med.* **31**, 154 (1994).
11. J. Kärger, H. Pfeifer, and W. Heink, *in* "Principles and Applications of Self-Diffusion Measurements by Nuclear Magnetic Resonance" (J. Waugh, Ed.), Vol. 1, Academic Press, San Diego, 1988.
12. P. M. Morse, and H. Feschbach, "Methods of Theoretical Physics," p. 997, McGraw–Hill, New York, 1953.
13. Y. C. Fung, "Foundations of Solid Mechanics," p. 525, Prentice-Hall, Englewood Cliffs, New Jersey, 1965.
14. C. Pierpaoli, P. Jezzard, and P. Basser, *in* "SMR/ESMRMB Joint Meeting, Nice, France, 1995," p. 899.
15. E. O. Brigham, "The Fast Fourier Transform and its Applications," p. 448, Prentice-Hall, Englewood Cliffs, New Jersey, 1988.
16. D. Marr, "Vision," Freeman, New York, 1982.
17. E. O. Stejskal and J. E. Tanner, *J. Chem. Phys.* **42**, 288 (1965).
18. D. G. Taylor and M. C. Bushell, *Phys. Med. Biol.* **30**, 345 (1985).
19. D. Le Bihan, E. Breton, D. Lallemand, P. Grenier, E. Cabanis, and M. Laval-Jeantet, *Radiology* **161**, 401 (1986).
20. P. J. Basser, J. Mattiello, and D. Le Bihan, *J. Magn. Reson. B* **103**, 247 (1994).

21. J. Mattiello, P. J. Basser, and D. LeBihan, *J. Magn. Reson. A* **108,** 131 (1994).
22. P. J. Basser and D. L. Bihan, Abstracts of the Society of Magnetic Resonance in Medicine, 11th Annual Meeting, Berlin, p. 1221, 1992.
23. L. Garrido, V. J. Wedeen, K. K. Kwong, U. M. Spencer, and H. L. Kantor, *Circ. Res.* **74,** 789 (1994).
24. Y. Yang, S. Xu, and M. J. Dawson, *Magn. Reson. Med.* **33,** 732 (1995).
25. C. E. Shannon and W. Weaver, "The Mathematical Theory of Communication," Univ. of Illinois Press, Urbana, Ilinois, 1963.
26. P. J. Basser, J. Mattiello, and D. LeBihan, Abstracts of the Society of Magnetic Resonance in Medicine, 11th Annual Meeting, Berlin, p. 1222, 1992.
27. P. Jezzard, and C. Pierpaoli, *in* "SMR/ESMRMB Joint Meeting, Nice, France, 1995," p. 903.
28. H. Jeffreys, "Cartesian Tensors," p. 93, Cambridge Univ. Press, Cambridge, Massachusetts, 1931.
29. K. Fukunaga, *in* "Introduction to Statistical Pattern Recognition" (H. G. Booker and N. DeClaris, Eds.), Academic Press, New York, 1972.
30. H. Goldstein, "Classical Mechanics," second ed., p. 672, Addison-Wesley, Reading, Massachusetts, 1980.